J|A|C|S ARTICLES

Published on Web 12/15/2009

Tyrosine Analogues for Probing Proton-Coupled Electron Transfer Processes in Peptides and Proteins

Susheel J. Nara,[†] Luca Valgimigli,*[,‡] Gian Franco Pedulli,[‡] and Derek A. Pratt*[,†]

Department of Chemistry, Queen's University, 90 Bader Lane, Ontario K7L 3N6, Canada, and Dipartimento di Chimica Organica "A. Mangini" Via San Giacomo 11, Università di Bologna, 40126, Bologna, Italy

Received September 17, 2009; E-mail: luca.valgimigli@unibo.it; pratt@chem.queensu.ca

Abstract: A series of amino acids analogous to tyrosine, but differing in the physicochemical properties of the aryl alcohol side chain, have been prepared and characterized. These compounds are expected to be useful in understanding the relationships between structure, thermodynamics, and kinetics in long-range proton-coupled electron transfer processes in peptides and proteins. Systematic changes in the acidity, redox potential, and O−H bond strength of the tyrosine side chain could be induced upon substituting the phenol for pyridinol and pyrimidinol moieties. Further modulation was possible by introducing methyl and *t*-butyl substitution in the position ortho to the phenolic hydroxyl. The unnatural amino acids were prepared by Pd-catalyzed cross-coupling of the corresponding halogenated aryl alcohol protected as their benzyl ethers with an organozinc reagent derived from *N*-Boc L-serine carboxymethyl ester. Subsequent debenzylation by catalytic hydrogenation yielded the tyrosine analogues in good yield. Spectrophotometric titrations revealed a decrease in tyrosine pK_a of ca. 1.5 log units per included nitrogen atom, along with a corresponding increase in the oxidation (peak) potentials of ca. 200 mV, respectively. All told, the six novel amino acids described here have phenol-like side chains with pK_a's that span a range of 7.0 to greater than 10, and an oxidation (peak) potential range of greater than 600 mV at and around physiological pH. Radical equilibration EPR experiments were carried out to reveal that the O−H bond strengths increase systematically upon nitrogen incorporation (by ca. 0.5−1.0 kcal/mol), and radical stability and persistence increase systematically upon introduction of alkyl substitution in the ortho positions. The EPR spectra of the aryloxyl radicals derived from tyrosine and each of the analogues could be determined at room temperature, and each featured distinct spectral properties. The uniqueness of their spectra will be helpful in discerning one type of aryloxyl in the presence of other possible aryloxyl radicals in peptides and proteins with multiple tyrosine residues between which electrons and protons can be transferred.

Introduction

Long-range electron transfer (ET) in peptides and proteins is now recognized as a common phenomenon, which plays a central role in processes as diverse as energy conversion (e.g., photosynthesis and respiration) and catalysis (e.g., ribonucleotide reduction and prostaglandin biosynthesis).[1] Early efforts to understand how the movement of charge between redox-active protein cofactors, or from a cofactor to a catalytic amino acid-derived radical, focused on characterizing the ability of the protein structure to act as a medium to facilitate tunneling.[2] From these studies, it was clear that ET through peptides and proteins decreases in rate in a logarithmic way with increasing distance between the electron donor and acceptor moieties and that this would make long-range ET in peptides and proteins too slow to be useful for either energy conversion or catalysis. This necessitates that long-range ET through peptides and proteins be rationalized on the basis of multiple ET steps via intervening redox-active amino acids, each one serving as an effective electron relay. Among the naturally occurring amino acids, tryptophan and tyrosine are most relevant as participants in the electron relay, due to their readily oxidizable indole and phenol side chains, respectively, and, of these two, tyrosine following its oxidation to the tyrosyl radical figures most prominently in both catalysis and energy conversion.[3]

The archetypical example of long-range ET mediated by intervening tyrosine (and tryptophan) residues occurs in the class I ribonucleotide reductase (RNR), which catalyzes the rate-limiting step of DNA biosynthesis in *E. coli* and other prokaryotes, reduction of ribonucleotides to deoxyribonucle-

[†] Queen's University.
[‡] Università di Bologna.

(1) See, for example: Cordes, M.; Giese, B. *Chem. Soc. Rev.* **2009**, *38*, 892–901. Giese, B.; Graber, M.; Cordes, M. *Curr. Opin. Chem. Biol.* **2008**, *12*, 755–759. Gray, H. B.; Winkler, J. R. *Proc. Natl. Acad. Sci. U.S.A.* **2005**, *102*, 3534–3539. Mose, C. C.; Page, C. C.; Dutton, P. L. *Curr. Opin. Chem. Biol.* **2003**, *7*, 551–556. Stubbe, J.; Nocera, D. G.; Yess, C. S.; Chang, M. C. Y. *Chem. Rev.* **2003**, *103*, 2167–2201, and references therein.

(2) See, for example: Gray, H. B.; Winkler, J. R. *Q. Rev. Biophys.* **2003**, *36*, 341–372, and references therein. Prytkova, T. R.; Kumikov, I. V.; Beratan, D. N. *Science* **2007**, *315*, 622–625.

(3) Stubbe, J.; van der Donk, W. A. *Chem. Rev.* **1998**, *98*, 705. Stubbe, J. *Chem. Commun.* **2003**, *20*, 2511. Pesavento, R. P.; van der Donk, W. A. *Adv. Protein Chem.* **2001**, *58*, 317.

(4) Sjöberg, B.-M.; Reichardt, P.; Gräslund, A.; Ehrenberg, A. A. *J. Biol. Chem.* **1978**, *253*, 6863–6865. Stubbe, J. *J. Biol. Chem.* **1990**, *265*, 5329–5332. Nordlund, P.; Sjöberg, B.-M.; Eklund, H. *Nature* **1990**, *345*, 593–598.

otides.[4] The catalytic cycle is initiated when the di-iron tyrosine (Y122) cofactor of one of the subunits of the enzyme (R2) oxidizes a cysteine residue on the other subunit (R1) located 35 Å away, prompting the suggestion that ET occurs in a stepwise fashion via the side chains of a tryptophan residue (W48) and three tyrosine residues (Y356, Y731, and Y730), which lie between the cofactor and the catalytic cysteine.[1,5] By studying the kinetic competence of RNR's wherein each of the tyrosine residues that form the putative ET relay were replaced with unnatural amino acids, which differed in their oxidation potentials (i.e., electron-poor such as **1**−**6**[6] and electron-rich such as **7**,[7] **8**[8]), Stubbe and co-workers were able to demonstrate that the redox chemistry of these intervening amino acid side chains is indeed involved in the radical propagation necessary for the initiation of catalysis.

Recent work by Gray and Winkler[9] as well as Giese and co-workers[10] has shone further light on the abilities of intermediate amino acid side chains to act as charge transfer relays. Of particular interest is the polypeptide model system of Giese and co-workers, which allows one to monitor charge migration between a 2,4-dialkoxyphenylalanine radical cation and a tyrosine residue via an intervening polyprolyl polypeptide of well-defined structure. By monitoring the change in charge migration as a function of intervening amino acid in the polyprolyl sequence, one can probe the role of the identity of the amino acid side chain on the kinetics of ET between donor and acceptor. Because the key thermodynamic parameter governing the rate of each of the intermediate ET steps in long-range ET is the redox potential of the amino acid side chain, which is intimately linked to its ability to give up a proton to the surrounding medium (which may be coupled to a proton transfer event involving another side chain presenting a basic or H-bond accepting site), it is highly desirable to use a series of amino acids that differ systematically in both their electron- and proton-donating abilities. However, due to the limited variability in the structural, acid−base, and redox properties of natural amino acids, the characteristics of the amino acids and their interactions with the surrounding medium (i.e., solvent, other amino acids, cofactors) that are important in maintaining effective long-range ET kinetics remain to be clearly elucidated.

While the work of Stubbe and co-workers has provided some examples of unnatural tyrosine analogues that could be useful in this regard (vide supra),[6] we sought to develop a series of unnatural amino acids whose acid−base, redox, and radical chemistry changed in a well-defined and systematic way, which could be relatively easily accessed by conventional synthetic methods and readily characterizable by EPR as well as UV spectroscopy. We conceptualized the incorporation of nitrogen atoms into the aromatic ring of tyrosine to construct pyridyl and pyrimidinyl analogues of tyrosine. The idea stemmed from our previous studies concerning the efficacy of 3-pyridinols and 5-pyrimidinols as radical-trapping antioxidants.[11] These previous investigations revealed that upon incorporation of a N-atom at the 3-position of phenol in lieu of the usual C-atom, the O−H bond dissociation enthalpy (BDE) increases by ∼1 kcal/mol, the ionization (oxidation) potential (IP) increases by a few 100 mVs, and the acidity also increases by ∼1.5 log units. With the second substitution of a N-atom, this time for the C-atom at the 5-position, the trend progressed in the same direction, increasing the bond strength, oxidation potential, and acidity even further. Thus, we expected that the O−H BDE, E^{o}, and pK_a of tyrosine could be varied in an isosteric manner by N-atom incorporation in the phenolic ring and that we could further substitute tyrosine and the pyridine and pyrimidine analogues in a systematic way to afford a series of unnatural amino acids, which may be exploited to help address some of the yet unanswered questions concerning long-range ET in peptides and proteins and the roles of tyrosyl radicals in energy conversion and catalysis.

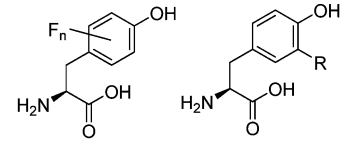

1 3-F
2 2,3-F_2
3 3,5-F_2
4 2,3,5-F_3
5 2,3,6-F_3
6 2,3,5,6-F_4

7 R = OH
8 R = NH_2

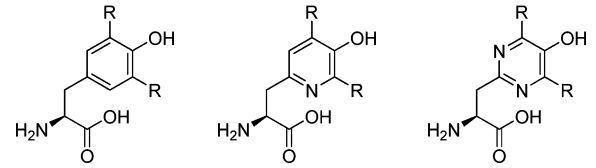

9 R = H (Tyr)
12 R= Me (mTyr)
15 R= *t*-Bu (bTyr)

10 R = H (Pyr)
13 R = Me (mPyr)

11 R = H (Pym)
14 R = Me (mPym)

Results

A. Synthesis. The preparation of the pyridyl (**10**) and pyrimidyl (**11**) analogues of tyrosine was carried out using an organozinc reagent derived from *N*-Boc protected L-serine methyl ester (**16**)[12] and 2-bromo-5-benzyloxy pyridine (**17**) and pyrimidine (**18**), respectively, as shown in Scheme 1. The pyridyl bromide **17** and the pyrimidyl bromide **18** were obtained from the corresponding pyridyl and pyrimidyl amines, both reported in a recent paper from our group,[11g] by nonaqueous halo-dediazoniation.[13] The Negeishi-type Pd-catalyzed cross-

(5) Uhlin, U.; Eklund, H. *Nature* **1994**, *370*, 533–539. Bennati, M.; Robblee, J. H.; Mugnaini, V.; Stubbe, J.; Freed, J. H.; Borbat, P. *J. Am. Chem. Soc.* **2005**, *127*, 15014–15015. Uppsten, M.; Färnegårdh, M.; Domkin, V.; Uhlin, U. *J. Mol. Biol.* **2006**, *359*, 365–377.
(6) (a) Seyedsayamdost, M. R.; Yee, C. S.; Reece, S. Y.; Nocera, D. G.; Stubbe, J. *J. Am. Chem. Soc.* **2006**, *128*, 1562–1568. (b) Seyedsayamdost, M. R.; Reece, S. Y.; Nocera, D. G.; Stubbe, J. *J. Am. Chem. Soc.* **2006**, *128*, 1569–1579. (c) Reece, S. Y.; Seyedsayamdost, M. R.; Stubbe, J.; Nocera, D. G. *J. Am. Chem. Soc.* **2006**, *128*, 13654–13655. (d) Reece, S. Y.; Seyedsayamdost, M. R.; Stubbe, J.; Nocera, D. G. *J. Am. Chem. Soc.* **2007**, *129*, 13828–13830.
(7) Seyedsayamdost, M. R.; Nocera, D. G. *J. Am. Chem. Soc.* **2006**, *128*, 2522–2523. Seyedsayamdost, M. R.; Chan, C. T. Y.; Mugnaini, V.; Stubbe, J.; Bennati, M. *J. Am. Chem. Soc.* **2007**, *129*, 15748–15749. Seyedsayamdost, M. R.; Stubbe, J. *J. Am. Chem. Soc.* **2007**, *129*, 2226–2227.
(8) Seyedsayamdost, M. R.; Xie, J.; Chan, C. T. Y.; Schultz, P. G.; Stubbe, J. *J. Am. Chem. Soc.* **2006**, *128*, 15060–15071.
(9) Shih, C.; Museth, A. K.; Abrahamsson, M.; Blanco-Rodriguez, A. M.; Di Billo, A. J.; Sudhamsu, J.; Crane, B. R.; Ronayne, K. L.; Towrie, M.; Vlcek, A.; Richards, J. H.; Winkler, J. R.; Gray, H. B. *Science* **2008**, *320*, 1760–1762.
(10) (a) Wang, M.; Gao, J.; Muller, P.; Giese, B. *Angew. Chem., Int. Ed.* **2009**, *48*, 4232–4234. (b) Giese, B.; Wang, M.; Gao, J.; Stoltz, M.; Muller, P.; Graber, M. *J. Org. Chem.* **2009**, *74*, 3621–3625. (c) Cordes, M.; Jacques, O.; Kottgen, A.; Jasper, C.; Boudebous, H.; Giese, B. *Adv. Synth. Catal.* **2008**, *350*, 1053–1062. (d) Cordes, M.; Kottgen, A.; Jasper, C.; Jacques, O.; Bodebous, H.; Giese, B. *Angew. Chem., Int. Ed.* **2008**, *47*, 3461–3463. (e) Giese, B.; Napp, M.; Jacques, O.; Boudebous, H.; Taylor, A. M.; Wirz, J. *Angew. Chem., Int. Ed.* **2005**, *44*, 4073–4075.

Scheme 1[a]

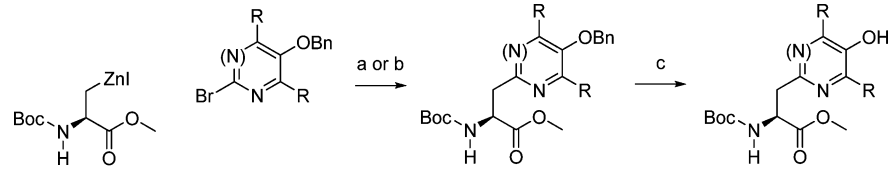

[a] Reagents and conditions: for **19** and **20**, (a) $PdCl_2(PPh_3)_2$, DMF, room temperature, 12 h; for **23** and **24**, (b) $Pd_2(dba)_3$, P(*o*-tolyl)$_3$, DMF, 50 °C, 12 h; (c) Pd−C, H_2, MeOH, room temperature, 12 h (abbreviations: pyr = pyridine; pym = pyrimidine).

Scheme 2[a]

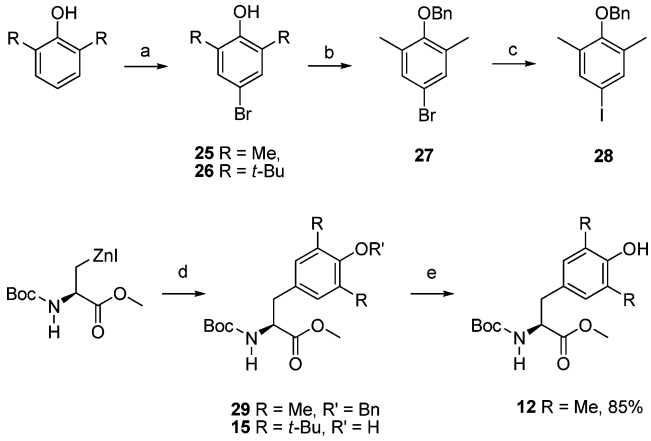

[a] Reagents and conditions: (a) NBS, MeCN, 12 h, reflux, 91% (R = Me), 85% (R = *t*-Bu), (b) BnBr, NaH, THF, room temperature, 12 h, 81%, (c) CuI, NaI, *N*,*N*-dimethylethylene diamine, 1,4-dioxane, reflux, 48 h, quant., (d) for **31**, **30**, $Pd_2(dba)_3$, P(*o*-tolyl)$_3$, DMF, 50 °C, 12 h, 48%; for **15**, **28**, $PdCl_2(PPh_3)_2$, 80 °C, 12 h, 22%, (e) Pd−C, H_2, MeOH, room temperature, 12 h, 85%.

coupling proceeded best with $PdCl_2(PPh_3)_2$ at room temperature in DMF. The next step, cleavage of the benzyl ethers of **19** and **20** to yield the aryl alcohols **10** and **11**, was easily accomplished by catalytic hydrogenation in MeOH and purified by flash column chromatography in good yield. This sequence was also employed in the preparation of the analogous pyridinol- and pyrimidinol-based amino acids featuring methyl substitution in the ortho positions relative to the phenolic hydroxyl. The cross-couplings of the more electron-rich methylated aryl bromides **21** and **22**, also prepared from the corresponding amines, proceeded best at slightly higher temperature (50 °C) with $Pd_2(dba)_3$/P(*o*-tolyl)$_3$ as the catalyst to give the benzyl-protected alcohols **23** and **24**, which were liberated to yield **13** and **14**.

The preparation of analogues of tyrosine with methyl and *tert*-butyl substitution in the ortho positions relative to the phenolic hydroxyl involved the same two-step Pd-catalyzed cross-coupling/catalytic hydrogenation sequence, following preparation of the appropriately substituted aryl halides (Scheme 2). Bromination of the commercially available 2,6-dialkylated phenols yielded the corresponding 4-bromophenols **25** and **26**, but while benzyl protection of the former was facile, benzylation of the latter proved cumbersome. Hence, the cross-coupling of **26** and **16** was carried out directly to yield **15**, albeit in low yield, while the methylated substrate **25** was coupled as the benzyl ether following a Cu-catalyzed Finkelstein reaction on **27**[14] to generate the more reactive aryl iodide coupling partner **28**. Subsequent removal of the benzyl group from **29** by catalytic hydrogenation yielded the ortho methylated tyrosine **12**.

B. Acid−Base Chemistry. The pK_a's of the tyrosine analogues (**10**−**15**) were determined using UV−vis spectroscopy and compared to that measured for tyrosine itself (**9**). To avoid complications arising from the free carboxylic acid and amino groups of the amino acid, they were left protected as the methyl ester and *tert*-butoxy carbamate groups, respectively. The UV spectra, which were recorded as a function of pH to obtain characteristic sigmoidal titration curves, revealed a slight red shift upon incorporation of N-atoms in the aromatic ring of tyrosine. Upon deprotonation, all of the derivatives exhibited a bathochromic shift, and from the changes in absorbance the fraction of the amino acid in its aryloxide ion form ($f_{aryloxide}$) was determined at different pH values. The pK_a values were then determined by plotting $f_{aryloxide}$ as a function of pH. The data are shown in Figure 1 along with the calculated pK_a values, which span a range of 7.0−10.7 for **9**−**14**. The pyridyl analogues **10** and **13** exhibited double sigmoidal curves due to protonation of the ring nitrogen at acidic pH. Introduction of nitrogen in tyrosine's phenolic ring lead to a decrease in the phenolic O−H pK_a of 1.9 on going from **9** to **10** and another 1.3 upon introduction of a second nitrogen on going from **10** to **11** (left panel of Figure 1). Methyl substitution raised the pK_a's of all of these analogues, by 0.5 and 0.3 for the phenol and pyrimidinol, respectively, and 1.3 for the pyridinol (right panel of Figure 1). The pK_a of the *tert*-butylated tyrosine analogue (**15**) was determined to be ∼13 in the same way (see Supporting Information).

C. Redox Chemistry. The oxidation (anodic) peak potentials (E_{pa}) of the tyrosine analogues (**10**−**15**) were determined as a function of pH in the physiologically relevant range of ∼6.0 to ∼9.0 using differential pulse voltammetry and, again, compared to the profile for tyrosine (**9**). The data are shown in Figure 2 and display a potential range from ∼250 to ∼950 mV for **9**−**14**

(11) (a) Pratt, D. A.; DiLabio, G. A.; Brigati, G.; Pedulli, G. F.; Valgimigli, L. *J. Am. Chem. Soc.* **2001**, *123*, 4625–4626. (b) Valgimigli, L.; Brigati, G.; Pedulli, G. F.; DiLabio, G. A.; Mastragostino, M.; Arbizzani, C.; Pratt, D. A. *Chem.-Eur. J.* **2003**, *9*, 4997–5010. (c) Wijtmans, M.; Pratt, D. A.; Valgimigli, L.; DiLabio, G. A.; Pedulli, G. F.; Porter, N. A. *Angew. Chem., Int. Ed.* **2003**, *42*, 4370–4373. (d) Wijtmans, M.; Pratt, D. A.; Brinkhorst, J.; Serwa, R.; Valgimigli, L.; Pedulli, G. F.; Porter, N. A. *J. Org. Chem.* **2004**, *69*, 9215–9223. (e) Kim, H.-Y.; Pratt, D. A.; Seal, J. R.; Wijtmans, M.; Porter, N. A. *J. Med. Chem.* **2005**, *48*, 6787–6789. (f) Nam, T.-G.; Rector, C. L.; Kim, H.-Y.; Sonnen, A. F.-P.; Meyer, R.; Werner, W. M.; Atkinson, J.; Rintoul, J.; Pratt, D. A.; Porter, N. A. *J. Am. Chem. Soc.* **2007**, *129*, 10211–10219. (g) Nara, S. J.; Jha, M.; Brinkhorst, J.; Zemanek, T. J.; Pratt, D. A. *J. Org. Chem.* **2008**, *73*, 9326–9333.
(12) Tabanella, S.; Valancogne, I.; Jackson, R. F. W. *Org. Biomol. Chem.* **2003**, *1*, 4254–4261.
(13) Francom, P.; Janeba, Z.; Shibuya, S.; Robins, M. J. *J. Org. Chem.* **2002**, *67*, 6788–6796.
(14) Klapars, A.; Buchwald, S. L. *J. Am. Chem. Soc.* **2002**, *124*, 14844–14845.

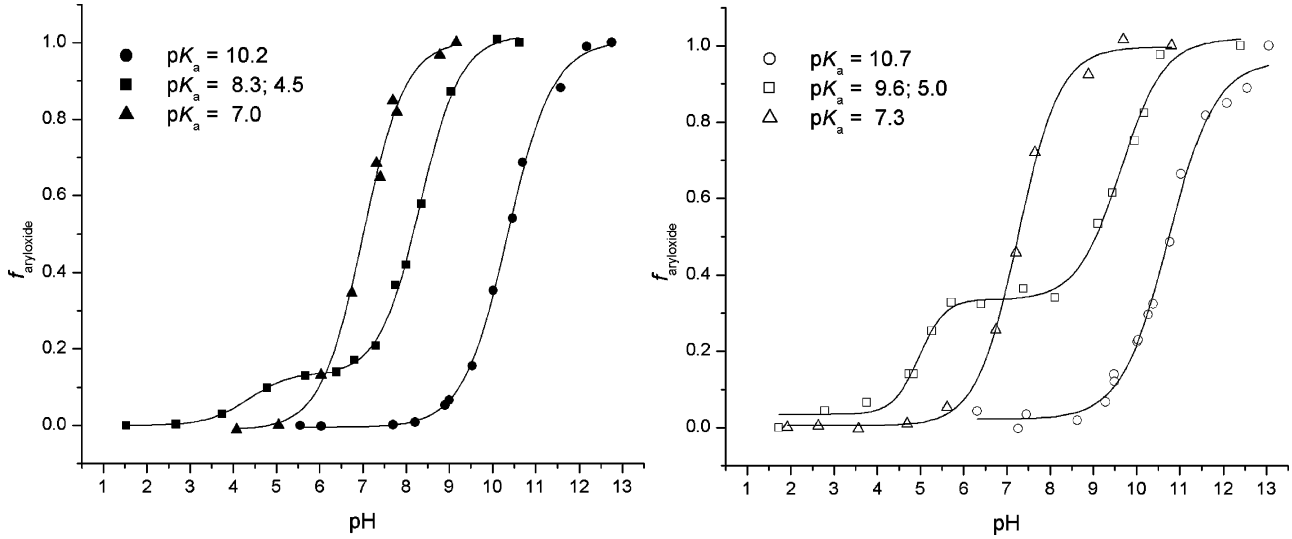

Figure 1. Fraction of aryloxide ion as a function of pH for tyrosine (●) and its analogues: **10** (■), **11** (▲), **12** (○), **13** (□), and **14** (△).

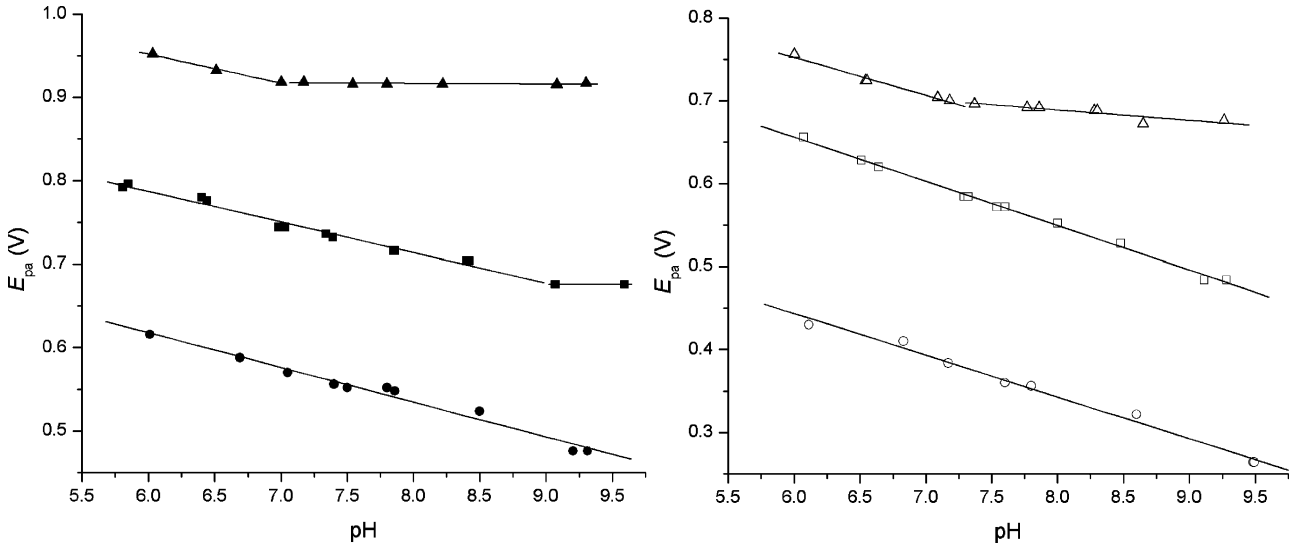

Figure 2. Oxidation (peak) potentials as a function of pH for tyrosine (●) and its analogues: **10** (■), **11** (▲), **12** (○), **13** (□), and **14** (△).

Table 1. EPR Spectral Parameters (HSC = Hyperfine Splitting Constants) for the Aryloxyl Radicals Derived From Tyrosine (**9**) and Its Analogues (**10**−**15**)

	HSCs ortho (G)	HSCs meta (G)	HSCs methylene (G)	*g*-factor
9	*a*(2H) 6.61	*a*(2H) 1.84	*a*(H) 7.29; *a*(H) 6.77	2.0048
10	*a*(H) 8.15; *a*(H) 5.5	*a*(N) 2.17; *a*(H) 1.40	*a*(H) 11.41; *a*(H) 7.7	2.0048
11	*a*(H) 8.65; *a*(H) 8.0	*a*(N) 2.75; *a*(N) 0.95	*a*(H) 10.72; *a*(H) 9.1	2.0049
12	*a*(6H) 6.50	*a*(2H) 1.77	*a*(H) 6.30; *a*(H) 6.35	2.0047
13	*a*(3H) 8.95; *a*(3H) 6.52	*a*(N) 2.20; *a*(H) 1.15	*a*(H) 10.32; *a*(H) 10.02	2.0048
14	*a*(6H) 6.84	*a*(2N) 1.86	*a*(H) 9.14; *a*(H) 9.12	2.0049
15	*a*(18H) ∼0.1	*a*(2H) 1.79	*a*(H) 7.10; *a*(H) 6.53	2.0046

over this pH range. Introduction of nitrogen in tyrosine's phenolic ring lead to an increase in E_{pa} of ca. 200 mV on going from **9** to **10** and another ca. 200 mV on going from **10** to **11** (left panel of Figure 2) and resulted in a leveling of the E_{pa}−pH profile for **10** and **11** once the pH reached the values of their phenolic pK_a's (vide supra). Methyl substitution lead to a systematic drop in E_{pa} values by roughly 150−200 mV on comparing **12**−**14** to **9**−**11** (right panel of Figure 2 to right panel of Figure 2). The corresponding potential range through the same pH range for the *tert*-butylated tyrosine analogue (**15**) was determined to be roughly 230−370 mV (see Supporting Information).

D. EPR Spectra. The EPR spectra of the aryloxyl radicals derived from the tyrosine analogues (**10**−**15**) were recorded upon exposure to a 10% v/v solution of di-*tert*-butyl peroxide in benzene, and compared to the spectrum derived from tyrosine (**9**) obtained under the same conditions. The spectral parameters are collected in Table 1. The *g*-factors, determined to be in the range of 2.0046−2.0049, were corrected with respect to 2,6-di-*tert*-butyl-4-methylphenol (or butylated hydroxytoluene, BHT)

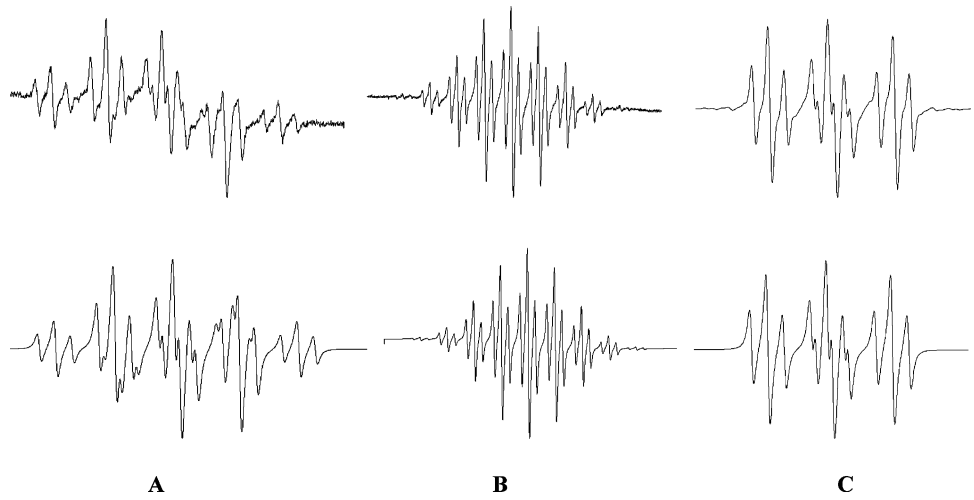

Figure 3. EPR spectra of the phenoxyl radicals derived from tyrosine (**9**), 3,5-dimethylated tyrosine (**12**), and 3,5-di-*tert*-butylated tyrosine (**15**) in benzene at 298 K and the corresponding simulated spectra.

and 3,5-di-*tert*-butylphenol, for which *g*-values of 2.0046 and 2.0048 are known, respectively.[15] The spectra for the series of aryloxyl radicals derived from **9**, **12** and **15** are shown as examples in Figure 3 (other representative spectra are included as Supporting Information). The increase in the persistence of the aryloxyl radicals upon introduction of methyl and *tert*-butyl groups in the ortho positions relative to the phenoxyl oxygen is clear from these spectra.

E. Radical Stability. The O−H bond dissociation enthalpies (BDEs) of the tyrosine analogues (**10**−**15**) were determined using the radical equilibration EPR (REqEPR) technique[15] and compared to that measured for tyrosine itself (**9**). The REqEPR technique relies on the generation of the aryloxyl radical derived from **9**−**15** in the presence of a reference compound of known O−H BDE close to that of the compound under investigation (within 2.5 kcal/mol), such that an equilibrium is established that reflects the difference in the strengths of the O−H bonds. The reference compounds used in these experiments were 2,6-di-*tert*-butyl-4-methylphenol (or butylated hydroxytoluene, BHT) and 3,5-di-*tert*-butylphenol, whose O−H BDEs are 79.9 ± 0.1 and 85.52 ± 0.3 kcal/mol,[15] respectively.[16] The EPR spectra recorded under these conditions are thus superpositions of the spectra of the two equilibrating aryloxyls, from which we can obtain the equilibrium constants. Assuming a negligible entropy change in the H-atom transfer reaction, the O−H BDEs can be calculated directly from the equilibrium constants. The O−H BDEs of **9**−**15**, the equilibrium constants from which they were derived, and the reference compounds used to establish the equilibria are given in Table 2.

Table 2. O−H Bond Dissociation Enthalpies in kcal/mol of Tyrosine (**9**) and Its Analogues (**10**−**15**) Determined by the Radical Equilibration EPR Technique with the Indicated Reference Compound

	reference	measured K_{eq} (±SD)	O−H BDE/kcal/mol[a]
9	3,5-di-*tert*-butylphenol	0.6 ± 0.1	85.2 ± 0.1
10	3,5-di-*tert*-butylphenol	5.2 ± 3.1	86.5 ± 0.6
11	3,5-di-*tert*-butylphenol	9.0 ± 6.7	86.8 ± 0.8
12	2,6-di-*tert*-butyl-4-methylphenol	12.6 ± 9.5	81.4 ± 0.8
13	2,6-di-*tert*-butyl-4-methylphenol	29.3 ± 3.9	81.9 ± 0.1
14	2,6-di-*tert*-butyl-4-methylphenol	57.6 ± 14.0	82.3 ± 0.2
15	2,6-di-*tert*-butyl-4-methylphenol	1.7 ± 0.3	80.2 ± 0.1

[a] Errors account for the SD in the measurement of K_{eq} and do not include the error in the reference BDE.

Discussion

The preparation and site-specific incorporation of unnatural amino acids into proteins is a very powerful approach to the study of a variety of protein-mediated biological processes, including catalysis and energy conversion, as well as protein folding,[17] ion channel function,[18] translation,[19] and signaling.[20] The adaptation of native chemical ligation to protein semisynthesis[21] has resulted in a veritable surge in the application of this approach to a variety of problems, one of the most interesting of which is radical transport in proteins,[1] a topic that has captured the fascination of many.

Our previous work on pyridinol and pyrimidinol antioxidants[11] led us to believe that pyridinol and pyrimidinol analogues of tyrosine could serve as useful alternatives to the fluorinated tyrosine analogues (**1**−**6**)[6] and 3-hydroxytyrosine (**7**)[7] and 3-aminotyrosine (**8**)[8] used by Stubbe, Nocera, and co-workers to study charge transport in peptides and proteins. From our previous work, we expected that the incorporation of nitrogen in the phenolic side chain of tyrosine would substantially lower the pK_a and elevate $E°$ and O−H BDE in a systematic way. The capability to modulate the electronic properties of the phenolic ring without the introduction of substituents onto the ring that may change the steric requirements of the side chain

(15) Lucarini, M.; Pedrielli, P.; Pedulli, G. F.; Cabiddu, S.; Fattuoni, C. *J. Org. Chem.* **1996**, *61*, 9259–9263. Lucarini, M.; Pedulli, G. F.; Cipollone, M. *J. Org. Chem.* **1994**, *59*, 5063–5070.

(16) The original values included in reference 15 have been given as 1.1 kcal/mol lower here according to the revised value of the O−H BDE in 2,4,6-tri-*tert*-butylphenol, see: Mulder, P.; Korth, H. G.; Pratt, D. A.; DiLabio, G. A.; Valgimigli, L.; Pedulli, G. F.; Ingold, K. U. *J. Phys. Chem. A* **2005**, *109*, 2647–2655.

(17) For example: Arnold, U.; Hinderaker, M. P.; Koditz, J.; Golbik, R.; Ulbrich-Hofmann, R.; Raines, R. T. *J. Am. Chem. Soc.* **2003**, *125*, 7500–7501.

(18) For example: Valiyaveetil, F. I.; Sekedat, M.; MacKinnon, R.; Muir, T. W. *Proc. Natl. Acad. Sci. U.S.A.* **2004**, *101*, 17045–17049.

(19) Maag, D.; Fekete, C. A.; Gryczynski, Z.; Lorsch, J. R. *Mol. Cell* **2005**, *17*, 265–275.

(20) For example: Lu, W.; Gong, D.; Bar-Sagi, D.; Cole, P. A. *Mol. Cell* **2001**, *8*, 759–769.

(21) Muir, T. W. *Annu. Rev. Biochem.* **2003**, *72*, 249–289. David, R.; Richter, M. P.; Beck-Sickinger, A. G. *Eur. J. Biochem.* **2004**, *271*, 663–677. Schwarzer, D.; Cole, P. A. *Curr. Opin. Chem. Biol.* **2005**, *9*, 561–569.

seemed ideal for the purpose of making unnatural tyrosine analogues for probing proton-coupled electron transfer reactions in peptides and proteins.

The preparation of the analogues was straightforward due to the work of Jackson and co-workers on the Pd-catalyzed arylation of an organozinc reagent derived from serine,[12] which was demonstrated to work well to attach various aryl moieties to the methylene adjacent the α carbon of the amino acid. While the isolated yields of the cross-coupling reactions are only moderate (ca. 60%), the sequence is scaleable, allowing gram quantities of the unnatural amino acids to be prepared, an important feature that allows facile preparation of the quantities required for introduction into model peptides by solid-phase peptide synthesis, and eventually for incorporation into proteins via expressed protein ligation.

The trends in physicochemical properties of tyrosine (Tyr) and its pyridine and pyrimidine analogues (hereafter Pyr and Pym) fit the expectations based on our earlier work. Upon introduction of nitrogen into the phenolic ring of Tyr in lieu of carbon at the 2- or 2- and 6-positions, the pK_a dropped by 1.9 and 3.2 log units, respectively. These effects are slightly larger than those obtained upon introduction of fluorine at either the 3- or 3- and 5-positions of tyrosine,[6b] which yield decreases of ~1.6 and ~2.8 log units, respectively, despite being further removed from the reactive hydroxyl moiety. The oxidation (peak) potentials also increase systematically along the Tyr/Pyr/Pym series by ca. 200 mV for each nitrogen at physiological pH. These differences are also greater than those seen in the fluorinated tyrosines,[6b] which are ca. 60 mV for the 3-F and then another 50 mV for the 3,5-F_2.

The EPR spectra of the aryloxyl radicals derived from Tyr and its pyridine and pyrimidine analogues could be determined at room temperature in benzene, and the resulting spectra were then used to determine the O−H BDEs of Tyr, Pyr, and Pym by the radical equilibration EPR technique. These experiments yielded an O−H BDE in tyrosine (protected as the N-Boc and carboxymethyl ester) of 85.2 ± 0.2 kcal/mol, 2 kcal/mol lower than the O−H BDE of phenol determined by the same method.[16] This value compares well with the only other value in the literature of 86.5 ± 0.5 kcal/mol determined from the pK_a of tyrosine and the one-electron reduction potential of the tyrosyl radical in water (the O−H BDE of phenol by this method is 88.2 ± 0.3 kcal/mol).[22] The pyridine and pyrimidine analogues have O−H BDEs that are higher by 1.2 and 1.6 kcal/mol, respectively. The increase in O−H BDE upon incorporation of the nitrogen atom(s) is consistent with our previous observations and is the result of their imparting greater electron poorness to any already electron-deficient aryloxyl radical.[11]

The vacant ortho positions of the phenolic rings of Tyr, Pyr, and Pym permit their further modification to systematically extend the range of structure−activity space that can be accessed by studies employing these analogues. The introduction of methyl substituents in these positions leads to unnatural amino acids (hereafter referred to as mTyr, mPyr, and mPym) with elevated pK_a's as compared to the unsubstituted analogues, slightly for the tyrosine and pyrimidine analogues (the pK_a's of Tyr and mTyr are 10.2 and 10.7, respectively; Pym and mPym are 7.0 and 7.3, respectively), but more so for the pyridine analogue (the pK_a's of Pyr and mPyr are 8.3 and 9.6, respectively). The origin of the greater susceptibility of the pyridine analogue of tyrosine to changes in the acidity of the O−H bond as a function of ortho methyl substitution is unclear, but, most importantly, the trends are maintained. The increase in pK_a upon methyl substitution can be rationalized by the destabilization of the aryloxide anion by the electron-donating methyl substituent groups. This also leads to lower oxidation potentials, roughly 200 mV lower for each of mTyr, mPyr, and mPym relative to Tyr, Pyr, and Pym, respecitvely, allowing a range of driving force of ca. 600 mV to be examined by the full set of analogues. The O−H BDEs also drop as a result of the electron donation of the methyl substituents, which stabilize the electron-poor aryloxyl radicals derived from the aryl alcohols. The difference is roughly 4 kcal/mol for each of the analogues.

The aryloxyl radicals derived from tyrosine and the analogues each have characteristic EPR spectra. The pyrimidinoxyl radicals derived from Pym and mPym are distinguished from the phenoxyl radicals derived from Tyr and mTyr due to their particular hyperfine splitting patterns, which include small couplings due to the ring nitrogens (a_N = 1.0−2.8 G). Interestingly, the pyrimidinoxyl radical derived from Pym is asymmetric on the EPR time scale, with the two ring nitrogens possessing distinctly different HSCs (and likewise the two ring protons). This may indicate either the formation of an intramolecularly-H-bonded structure, wherein one of the pyrimidine nitrogen atoms is H-bonded to the amide N−H proton in a six-membered ring conformation, or the restricted rotation of the pyrimidine ring about the bond connecting C2 of the pyrimidine ring and the benzyl-like carbon. The former explanation is supported by the different magnitudes of the ring nitrogen couplings, which are consistent with increased (negative) spin density in the H-bonded position, while decreasing the spin density at the counterlateral ring position. Of course, while this interaction may be important in an isolated molecule in a non-H-bond donating solvent, it is unclear if it would be observed in a peptide or protein, providing nonetheless a potential source of information (vide infra). Perhaps more significantly, the benzyl-like diastereotopic hydrogens have different HSCs (this is clearly supported by the corresponding second derivative spectra; see Supporting Information for an example), and these are 2−4 G larger for the pyrimidinoxyl radicals derived from Pym (9.1, 10.72 G) and mPym (9.14, 9.12 G) than for the phenoxyls derived from Tyr (7.29, 6.77 G) and mTyr (6.30, 6.35 G), reflecting the greater electron deficiency of the pyrimidine ring. These couplings will allow for the unambiguous assignment of a tyrosyl radical containing these heteroatoms.

The spectra of the pyridinoxyl radicals derived from Pyr and mPyr are more complicated than either the phenoxyls or the pyrimidinoxyls due to their asymmetry. Nevertheless, their EPR spectra could be deconvoluted and the HSCs determined by comparison with simulated spectra (see Supporting Information). As for the pyrimidinoxyl radicals, the HSCs of the diastereotopic benzylic H-atoms were characteristically larger for the pyridinoxyl radicals when compared to the phenoxyl radicals, with values of 7.7 and 11.4 G for Pyr, and 10.32 and 10.02 G for mPyr, respectively. Of course, intramolecular H-bonding between the ring nitrogen and amide N−H is expected to be more prominent in pyridinoxyl radicals, which contain a more basic

(22) Using pulse radiolytic techniques to obtain a reversible potential as in: Lind, J.; Shen, X.; Eriksen, T. E.; Merényi, G. *J. Am. Chem. Soc.* **1990**, *112*, 479–482. It is important to note that the determination of accurate O−H BDEs for these analogues allows for a better rationalization of the effect of changes in driving force on changes in the kinetics of PCET processes. Because the electrochemistry of the tyrosyl/tyrosinate redox couples measured here, and also of the fluorinated tyrosine analogues,[6b] is irreversible, thermodynamic data cannot be cleanly extracted.

ring nitrogen, than in the case of the pyrimidinoxyl radicals, thereby leading to larger HSCs upon H-bond formation. Indeed, the a_N values of 2.17 and 2.20 G measured for pyridinoxyl radicals from **10** and **13**, respectively, are in agreement with this expectation.

Rationalization of the complex and distinctive hyperfine pattern of the aryloxyl radicals derived from tyrosine and its pyridine and pyrimidine analogues is an important step toward the use of these unnatural amino acids to probe proton-coupled electron transfer processes along peptide chains. Indeed, the relative persistence of these aryloxyl radicals, particularly those bearing either methyl or *tert*-butyl substituents, will allow room temperature EPR investigations of the peptides into which they will be inserted, enabling one to unambiguously assign the position of the unpaired electron on the basis of the relevant spectral differences among the aryloxyl radicals. The larger coupling constants of the benzyl-like methylenic hydrogens for the pyridinoxyl and pyrimidinoxyl radicals allow for their clear distinction from phenoxyl radicals; furthermore, the hyperfine pattern due to paramagnetic nuclei in *meta*-positions (^{1}H $S = 1/2$, or ^{14}N $S = 1$) is distinctive even when similar HSC are displayed (e.g., **9** $a(2H_m)$ 1.84 G vs **14** a(2N) 1.86 G). As discussed, intramolecular H-bonding in aryloxyl radicals derived from compounds **10**, **11**, and **13** is clearly detectable in the EPR spectra from variation of the spin density at the corresponding positions. While this results in nonequivalence of the two meta (and consequently ortho) positions, complicating the spectra and reducing their intensity, it will also provide an excellent tool to probe the cybotactic region and the occurrence of intermolecular H-bonding in the corresponding sites of a peptide incorporating such unnatural amino acids. Even the disappearance of such intramolecular interaction upon incorporation of the amino acid in the peptide would turn into a valuable source of information.

Conclusions

Unnatural amino acids containing phenol, 3-pyridinol, and 5-pyrimidinol side chains have been synthesized by Pd-catalyzed cross-couplings of appropriately substituted haloaryl benzyl ethers and an organozinc reagent derived from serine followed by catalytic hydrogenation. The pK_a's and oxidation (peak) potentials of the analogues reveal that a wide range in both proton- and electron-donor ability can be accessed by these unnatural amino acids as a function of both incorporation of nitrogen in the phenolic ring and introduction of methyl substituents on the phenolic ring. The EPR spectra of the aryloxyl radicals generated from these analogues are characterized by different signals, which could be useful in distinguishing between tyrosyl radicals and the aryloxyl radicals derived from its analogues, some of which differ considerably in their stability, as revealed by radical equilibration EPR experiments used to determine the O−H BDEs in tyrosine as well as the newly synthesized analogues.

While our motivation for carrying out this work is to help clarify the role of coupling of proton and electron transfer in charge transport processes in peptides and proteins, it should be pointed out that the unnatural amino acids reported here are likely to be helpful in exploring other phenomena. For example, Kim and Cole[23] employed the fluorinated tyrosine analogues **1**−**6** in mechanistic studies of protein tyrosine kinase-catalyzed phosphoryl transfer reactions. One can envision still other uses for our newly prepared analogues in mechanistic studies where systematic changes in the side chain acidity, oxidizability, radical stability, nucleophilicity, and nucleofugality are desired.

(23) Kim, K.; Cole, P. A. *J. Am. Chem. Soc.* **1998**, *120*, 6851–6858.

Experimental Section

Materials and Methods. All reagents were purchased from commercial sources and used without further purification, unless otherwise indicated. Column chromatography was carried out using Silica-P Flash silica gel (60 Å 40−63 μm, 500 m^2/g) from Silicycle. ^{1}H NMR and ^{13}C NMR spectra were recorded at 25 °C on a Bruker Avance spectrometer at 400 and 100 MHz, respectively. Mass spectra were obtained on an Applied Biosystems/MDS Sciex QSTAR XL QqTOF mass spectrometer. EPR spectra were recorded on a Bruker Elexsys 500 equipped with a Super X-Band ER049 microwave bridge, FF-lock, and Gauss-meter for accurate field calibration and g-factor measurement.

General Procedure for Bromo-dediazoniation. To a solution of 5-benzyloxy-2-aminopyri(mi)dine (2.27 mmol) in 20 mL of dry dibromomethane was added benzyltrimethylammonium bromide (10.22 mmol, 4.5 equiv) followed by dropwise addition of *tert*-butylnitrite (22.73 mmol, 10 equiv). The solution was stirred at room temperature under nitrogen atmosphere and was monitored on TLC. The reaction times ranged from 1 to 12 h depending on the nucleophilicity of the amine. Upon completion, the reaction was quenched by addition of aqueous $NaHCO_3$ solution, and the product was extracted with dichloromethane. The combined organic extracts were washed with brine, dried over Na_2SO_4, and concentrated in vacuo. The residue was subjected to flash chromatography (eluent: ethyl acetate/hexanes). The purified product was characterized by ^{1}H NMR, ^{13}C NMR, and mass spectrometry.

5-Benzyloxy-2-bromopyridine (17). Yield: 45%. ^{1}H NMR (400 MHz, $CDCl_3$): δ 8.15 (d, $J = 3.2$ Hz, 1H, arom.), 7.43−7.37 (m, 6H, arom.), 7.17 (dd, $J = 8.8$, 3.2 Hz, 1H, arom.), 5.11 (s, 2H, −CH2) ppm. ^{13}C NMR (100 MHz, $CDCl_3$): δ 154.61, 137.90, 135.62, 132.42, 128.81, 128.51, 128.19, 127.54, 125.32, 70.77 ppm. HRMS (ES+) calculated (M) 262.9946, observed 262.9946.

5-Benzyloxy-2-bromopyrimidine (18). Yield: 36%. ^{1}H NMR (400 MHz, $CDCl_3$): δ 8.31 (s, 2H, arom.), 7.43−7.40 (m, 5H, arom.), 5.16 (s, 2H, −CH2) ppm. ^{13}C NMR (100 MHz, $CDCl_3$): δ 152.44, 146.74, 142.97, 134.68, 128.97, 128.90, 127.65, 71.23 ppm. HRMS (ES+) calculated (M) 265.9878, observed 265.9877.

(2*S*)-(*N*-*tert*-Butoxycarbonylamino)-3-(5′-benzyloxypyrid-2′-yl)-propionic Acid Methyl Ester (19). To a flame-dried Schlenk flask was weighed zinc powder (3.46 mmol, 0.226 g), and then it was dried by heating it with a heat gun under vacuum. Iodine (0.076 mmol, 0.02 g) was then added to the dried zinc powder under nitrogen. The flask was then heated with heat gun while under high vacuum for 10 min for activation. The flask containing zinc slurry was then cooled to 0 °C in an ice bath, and to it a solution of iodoserine (1.153 mmol, 0.380 g) in DMF (3 mL) was added dropwise and stirred at room temperature for 90 min for Zn insertion. To this solution of organozinc compound were then added 2-bromo-5-benzyloxypyridine (1.534 mmol, 0.406 g) and $PdCl_2(PPh_3)_2$ (0.062 mmol, 0.044 g), and they were stirred at room temperature overnight. The reaction mixture was diluted with ethyl acetate and washed with water and brine. The combined organic extracts were dried over Na_2SO_4 and concentrated in vacuo. The crude oil was subjected to flash chromatography (eluent: ethyl acetate/hexanes) to yield 58%. ^{1}H NMR (400 MHz, $CDCl_3$): δ 8.30 (d, $J = 2.8$ Hz,1H, arom.), 7.44−7.36 (m, 5H, arom.), 7.21−7.18 (dd, $J = 8.8$, 3.2 Hz, 1H, arom.), 7.06 (d, $J = 8.4$ Hz, 1H, arom.), 5.82 (d, 1H, $J = 7.2$ Hz, 1H, −NH), 5.10 (s, 2H, $-CH_2$), 4.67−4.64 (m, 1H, −CH), 3.70 (s, 3H, $-OCH_3$), 3.27 (dd, $J = 14.8$, 6.0 Hz, 1H, HCH), 3.21 (dd, $J = 14.8$, 4.8 Hz, 1H, HCH), 1.44 (s, 9H, $-C(CH_3)_3$) ppm. ^{13}C NMR (100 MHz, $CDCl_3$): δ 172.51, 155.50, 153.71, 149.36, 137.42, 136.19, 128.72, 128.30, 127.52, 123.87, 122.37, 79.69, 70.44, 53.28, 52.22, 38.45, 28.33 ppm. HRMS (ES+) calculated (M) 386.1842, observed 386.1852.

(2*S*)-(*N*-*tert*-Butoxycarbonylamino)-3-(5′-benzyloxypyrimid-2′-yl)-propionic Acid Methyl Ester (20). The organozinc reagent (1.153 mmol) was prepared in the same way as described for pyridyl analogue. To the solution of organozinc compound were then added 2-bromo-5-benzyloxypyrimidine (1.534 mmol, 0.408 g) and $PdCl_2(PPh_3)_2$ (0.062 mmol, 0.044 g), and the mixture was stirred at 50 °C overnight. The reaction mixture was diluted with ethyl acetate and washed with water and brine. The combined organic extracts were dried over Na_2SO_4 and concentrated in vacuo. The crude oil was subjected to flash chromatography (eluent: ethyl acetate/hexanes) to yield 55% and was characterized by ^{1}H NMR, ^{13}C NMR, and mass spectrometry. ^{1}H NMR (400 MHz, $CDCl_3$): δ 8.38 (s, 2H, arom.), 7.42−7.35 (m, 5H, arom.), 5.84 (d, 1H, J = 8.4 Hz, 1H, −NH), 5.13 (s, 2H, $-CH_2$), 4.80−4.76 (m, 1H, −CH), 3.69 (s, 3H, $-OCH_3$), 3.50 (dd, J = 15.4, 5.4 Hz, 1H, HCH), 3.37 (dd, J = 15.4, 4.6 Hz, 1H, HCH), 1.43 (s, 9H, $-C(CH_3)_3$) ppm. ^{13}C NMR (100 MHz, $CDCl_3$): δ 172.45, 159.46, 155.51, 151.16, 144.16, 135.31, 128.85, 128.65, 127.59, 79.74, 70.80, 52.30, 52.12, 39.79, 28.32 ppm. HRMS (ES+) calculated (M) 387.1794, observed 387.1791.

General Procedure for Hydrogenolysis of 5-Benzyloxy Derivatives of Pyri(mi)dines. A solution of benzyloxy protected amino acid (0.545 mmol, 0.211 g) in 10 mL of MeOH was treated with 5% Pd on C (0.04 g), and the resulting black suspension was stirred at room temperature under H_2 atmosphere (1 atm) overnight. The catalyst was removed by filtration through a pad of Celite, and filtrate was concentrated under reduced pressure. The residue was subjected to flash chromatography (eluent: ethyl acetate/hexanes). The purified product was characterized by ^{1}H NMR, ^{13}C NMR, and mass spectrometry. Although the conversion was quantitative in all of the cases, the purification and isolation of the polar derivatives led to slightly reduced yields.

Compound 10. Yield: 81%. ^{1}H NMR (400 MHz, $CDCl_3$): δ 8.17 (s, 1H), 7.19 (d, J = 8 Hz, 1H), 7.08 (d, J = 8 Hz, 1H), 5.75 (d, J = 8 Hz, 1H), 4.67 (bs, 1H), 3.72 (s, 3H), 3.22 (m, 2H), 1.41 (s, 9H) ppm. ^{13}C NMR (100 MHz, $CDCl_3$): δ 172.73, 155.58, 152.42, 147.67, 136.74, 124.63, 124.46, 80.08, 53.51, 52.50, 38.36, 28.29 ppm. HRMS (ES+) calculated (M) 296.1372, observed 296.1377.

Compound 11. Yield: 82%. ^{1}H NMR (400 MHz, $CDCl_3$): δ 9.34 (bs, 1H), 8.30 (s, 2H), 5.95 (d, J = 8.4 Hz, 1H), 4.79−4.81 (m, 1H), 3.71 (s, 3H), 3.44 (dd, J = 15.4, 5.8 Hz, 1H), 3.36 (dd, J = 15.0, 4.2 Hz, 1H), 1.42 (s, 9H) ppm. ^{13}C NMR (100 MHz, $CDCl_3$): δ 172.93, 157.53, 155.93, 150.26, 144.69, 80.51, 52.67, 52.35, 39.55, 28.31 ppm. HRMS (ES+) calculated (M) 297.1325, observed 297.1323.

5-Benzyloxy-2-bromo-4,6-dimethylpyridine (21). Yield: 33%. ^{1}H NMR (400 MHz, $CDCl_3$): δ 7.43−7.36 (m, 5H, arom.) 7.14 (s, 1H, arom.), 4.81 (s, 2H, $-CH_2$), 2.48 (s, 3H, $-CH_3$), 2.22 (s, 3H, $-CH_3$) ppm. ^{13}C NMR (100 MHz, $CDCl_3$): δ 153.69, 151.89, 143.55, 136.46, 134.93, 128.70, 128.49, 128.05, 127.66, 74.85, 19.38, 15.95 ppm. HRMS (ES+) calculated (M) 291.0259, observed 291.0249.

5-Benzyloxy-2-bromo-4,6-dimethylpyrimidine (22). Yield: 33%. ^{1}H NMR (400 MHz, $CDCl_3$): δ 7.43−7.41 (m, 5H, arom.), 4.88 (s, 2H, $-CH_2$), 2.44 (s, 6H, 2 × $-CH_3$) ppm. ^{13}C NMR (100 MHz, $CDCl_3$): δ 163.90, 149.87, 145.21, 135.61, 128.89, 128.86, 128.29, 75.60, 19.14 ppm. HRMS (ES+) calculated (M) 292.0211, observed 292.0208.

(2*S*)-(*N*-*tert*-Butoxycarbonylamino)-3-(5′-benzyloxy-4′,6′-dimethylpyrid-2′-yl)-propionic Acid Methyl Ester (23). The organozinc reagent (1.153 mmol) was prepared in the same way as described for pyri(mi)dyl analogues. To the solution of organozinc compound were then added 2-bromo-5-benzyloxy-4,6-dimethylpyridine (1.534 mmol, 0.450 g), P(*o*-tolyl)$_3$ (0.125 mmol, 0.038 g), and Pd_2dba_3 (0.062 mmol, 0.057 g), and the mixture was stirred at 50 °C overnight. The reaction mixture was diluted with ethyl acetate and washed with water and brine. The combined organic extracts were dried over Na_2SO_4 and concentrated in vacuo. The crude oil was subjected to flash chromatography (eluent: ethyl acetate/hexanes) to yield 57% and was characterized by ^{1}H NMR, ^{13}C NMR, and mass spectrometry. ^{1}H NMR (400 MHz, $CDCl_3$): δ 7.45−7.34 (m, 5H, arom.), 6.81 (s, 1H, arom.), 5.89 (d, 1H, J = 7.6 Hz, 1H, −NH), 4.81 (s, 2H, $-CH_2$), 4.64 (m, 1H, −CH), 3.71 (s, 3H, $-OCH_3$), 3.22 (dd, J = 14.4, 5.6 Hz, 1H, HCH), 3.14 (dd, J = 14.6, 4.6 Hz, 1H, HCH), 2.47 (s, 3H, $-CH_3$), 2.23 (s, 3H, $-CH_3$), 1.44 (s, 9H, $-C(CH_3)_3$) ppm. ^{13}C NMR (100 MHz, $CDCl_3$): δ 172.55, 155.52, 151.68, 151.24, 150.92, 140.49, 136.92, 128.61, 128.27, 127.91, 124.03, 79.58, 74.55, 53.19, 52.15, 38.43, 28.34, 19.55, 15.95 ppm. HRMS (ES+) calculated (M) 414.2155, observed 414.2153.

(2*S*)-(*N*-*tert*-Butoxycarbonylamino)-3-(5′-benzyloxy-4′,6′-dimethylpyrimidin-2′-yl)-propionic Acid Methyl Ester (24). The organozinc reagent (1.153 mmol) was prepared in the same way as described for pyri(mi)dyl analogues. To the solution of organozinc compound were then added 2-bromo-5-benzyloxy-4,6-dimethylpyrimidine (1.153 mmol, 0.339 g), P(*o*-tolyl)$_3$ (0.125 mmol, 0.038 g), and Pd_2dba_3 (0.062 mmol, 0.057 g), and the mixture was stirred at 50 °C overnight. The reaction mixture was diluted with ethyl acetate and washed with water and brine. The combined organic extracts were dried over Na_2SO_4 and concentrated in vacuo. The crude oil was subjected to flash chromatography (eluent: ethyl acetate/hexanes) to yield 57% and was characterized by ^{1}H NMR, ^{13}C NMR, and mass spectrometry. ^{1}H NMR (400 MHz, $CDCl_3$): δ 7.38−7.34 (m, 5H, arom.), 5.82 (d, 1H, J = 8.4 Hz, 1H, −NH), 4.81 (s, 2H, $-CH_2$), 4.77−4.74 (m, 1H, −CH), 3.68 (s, 3H, $-OCH_3$), 3.43 (dd, J = 15.8, 5.4 Hz, 1H, HCH), 3.28 (dd, J = 15.6, 4.4 Hz, 1H, HCH), 2.38 (s, 6H, 2 × $-CH_3$), 1.42 (s, 9H, $-C(CH_3)_3$) ppm. ^{13}C NMR (100 MHz, $CDCl_3$): δ 172.49, 160.82, 160.19, 155.50, 148.57, 136.14, 128.71, 128.58, 128.09, 79.65, 75.19, 52.21, 52.01, 39.97, 28.34, 19.07 ppm. HRMS (ES+) calculated (M) 415.2107, observed 415.2121.

Compound 13. Yield: 75%. ^{1}H NMR (400 MHz, $CDCl_3$): δ 6.84 (s, 1H), 5.95 (d, J = 8 Hz, 1H), 4.61 (d, J = 4 Hz, 1H), 3.73 (s, 3H), 3.19 (m, 2H), 2.45 (s, 3H), 2.25 (s, 3H), 1.43 (s, 9H) ppm. ^{13}C NMR (100 MHz, $CDCl_3$): δ 172.53, 155.63, 148.80, 146.30, 143.66, 134.65, 124.27, 79.79, 53.55, 52.31, 37.60, 28.33, 18.39, 15.92 ppm. HRMS (ES+) calculated (M) 324.1685, observed 324.1686.

Compound 14. Yield: 88%. ^{1}H NMR (400 MHz, $CDCl_3$): δ 5.95 (d, 1H, J = 8.0 Hz, 1H), 4.74−4.72 (m, 1H), 3.70 (s, 3H), 3.40 (dd, J = 15.4, 5.4 Hz, 1H), 3.26 (dd, J = 15.4, 4.6 Hz, 1H), 2.40 (s, 6H), 1.42 (s, 9H) ppm. ^{13}C NMR (100 MHz, $CDCl_3$): δ 172.77, 156.55, 155.73, 153.32, 146.22, 80.01, 52.38, 52.24, 39.23, 28.31, 18.64 ppm. HRMS (ES+) calculated (M) 325.1638, observed 325.1647.

4-Bromo-2,6-dimethylphenol (25). To the solution of 2,6-dimethylphenol (16.37 mmol, 2.00 g) in acetonitrile (20 mL) was added NBS (17.189 mmol, 3.06 g), and it was refluxed overnight. After the completion of reaction as indicated by TLC, the reaction mixture was concentrated under reduced pressure and residue reconstituted in ethyl acetate. The organic solution was washed with water and brine. The combined organic extracts were dried over Na_2SO_4 and concentrated in vacuo. The crude residue was subjected to flash chromatography (eluent: ethyl acetate/hexanes) to yield 91%. ^{1}H NMR (400 MHz, $CDCl_3$): δ 7.13 (s, 2H), 4.69 (s, 1H), 2.24 (s, 6H) ppm. ^{13}C NMR (100 MHz, $CDCl_3$): δ 151.32, 131.02, 125.27, 112.04, 15.78 ppm. HRMS (ES+) calculated (M) 199.9837, observed 199.9831.

4-Bromo-2,6-di-*tert*-butylphenol (26). To the solution of 2,6-di-*tert*-butylphenol (9.709 mmol, 2.00 g) in acetonitrile (20 mL) was added NBS (10.194 mmol, 1.814 g), and it was refluxed overnight. After the completion of reaction as indicated by TLC, the reaction mixture was concentrated under reduced pressure and residue reconstituted in ethyl acetate. The organic solution was washed with water and brine. The combined organic extracts were dried over Na_2SO_4 and concentrated in vacuo. The crude residue was subjected to flash chromatography (eluent: ethyl acetate/hexanes) to yield 85%. ^{1}H NMR (400 MHz, $CDCl_3$): δ 7.28 (s, 2H), 5.19 (s, 1H),

1.44 (s, 18H) ppm. ^{13}C NMR (100 MHz, $CDCl_3$): δ 152.92, 138.18, 127.85, 112.62, 34.50, 30.07 ppm. HRMS (ES+) calculated (M) 284.0776, observed 284.0782.

2-Benzyloxy-5-bromo-1,3-dimethylbenzene (27). To the solution of 4-bromo-2,6-dimethylphenol (8.409 mmol, 1.7 g) in dry tetrahydrofuran (20 mL) was added sodium hydride (9.249 mmol, 0.37 g), and the mixture was stirred for 5 min. The vigorous evolution of hydrogen gas was observed. To the resulting suspension was added benzyl bromide (9.249 mmol, 1.124 mL) dropwise, and the mixture was stirred at room temperature overnight. After the completion of reaction as indicated by TLC, the reaction was quenched by addition of aqueous saturated NH_4Cl solution. The solvent was removed under reduced pressure, and residual oil was diluted with ethyl acetate. The organic layer was washed with 1% HCl solution, water, and brine. The combined organic extracts were dried over Na_2SO_4 and concentrated in vacuo. The crude residue was subjected to flash chromatography (eluent: ethyl acetate/hexanes) to yield 81%. ^{1}H NMR (400 MHz, $CDCl_3$): δ 7.49−7.38 (m, 5H, arom.), 7.19 (s, 2H, arom.), 4.81 (s, 2H, $-CH_2$), 2.29 (s, 6H, 2 × $-CH_3$) ppm.^{13}C NMR (100 MHz, $CDCl_3$): δ 154.90, 137.26, 133.39, 131.49, 128.58, 128.15, 127.85, 116.53, 74.18, 16.27 ppm. HRMS (ES+) calculated (M) 290.0306, observed 290.0302.

2-Benzyloxy-5-iodo-1,3-dimethylbenzene (28). Yield: 79%. ^{1}H NMR (400 MHz, $CDCl_3$): δ 7.47−7.39 (m, 7H), 4.80 (s, 2H), 2.27 (s, 6H) ppm. ^{13}C NMR (100 MHz, $CDCl_3$): δ 155.77, 137.59, 137.23, 133.80, 128.59, 128.16, 127.85, 87.88, 74.16, 16.08 ppm. HRMS (ES+) calculated (M) 338.0168, observed 338.0164.

(2*S*)-(*N*-*tert*-Butoxycarbonylamino)-3-(2′-benzyloxy-1′,3′-dimethylphen-5′-yl)-propionic Acid Methyl Ester (29). The organozinc reagent (1.153 mmol) was prepared in the same way as described for pyri(mi)dyl analogues. To the solution of organozinc compound were then added 5-benzyloxy-2-iodo-4,6-dimethylbenzene (1.153 mmol, 0.390 g), P(*o*-tolyl)$_3$ (0.125 mmol, 0.038 g), and $PdCl_2$ (0.062 mmol, 0.011 g), and the mixture was stirred at 50 °C for 1 h. The reaction mixture was diluted with ethyl acetate and washed with water and brine. The combined organic extracts were dried over Na_2SO_4 and concentrated in vacuo. The crude oil was subjected to flash chromatography (eluent: ethyl acetate/hexanes) to yield 48%. ^{1}H NMR (400 MHz, $CDCl_3$): δ 7.40−7.33 (m, 2H), 7.31−7.26 (m, 3H), 6.70 (s, 2H), 4.91 (d, J = 8 Hz, 1H), 4.71 (s, 2H), 4.45−4.42 (m, 1H), 3.64 (s, 3H), 2.93 (dd, J = 16.0, 8.0 Hz, 1H), 2.85 (dd, J = 16.0, 8.0 Hz, 1H), 2.18 (s, 6H), 1.35 (s, 9H) ppm. ^{13}C NMR (100 MHz, $CDCl_3$): δ 171.50, 154.10, 153.76, 136.63, 130.39, 130.06, 128.68, 127.48, 126.93, 126.72, 78.83, 72.93, 53.49, 51.09, 36.61, 27.29, 15.38 ppm. HRMS (ES+) calculated (M) 413.2202, observed 413.2184.

Compound 12. Yield: 85%. ^{1}H NMR (400 MHz, $CDCl_3$): δ 6.73 (s, 2H), 5.00 (d, J = 8.0 Hz, 1H), 4.52 (d, J = 8.0 Hz, 1H), 3.74 (s, 3H), 2.98−2.92 (m, 2H), 2.21 (s, 6H), 1.44 (s, 9H) ppm. ^{13}C NMR (100 MHz, $CDCl_3$): δ 172.67, 155.14, 151.30, 129.39, 127.32, 123.09, 79.86, 54.63, 52.12, 37.39, 28.32, 15.91 ppm. HRMS (ES+) calculated (M) 323.1733, observed 323.1732.

Compound 15. The organozinc reagent (1.029 mmol) was prepared in the same way as described for pyri(mi)dyl analogues. To the solution of organozinc compound were then added 4-bromo-2,6-di-*tert*-butylphenol (0.776 mmol, 0.222 g) and $PdCl_2(PPh_3)_2$ (0.055 mmol, 0.039 g), and the mixture was stirred at 80 °C for 12 h. The reaction mixture was diluted with ethyl acetate and washed with water and brine. The combined organic extracts were dried over Na_2SO_4 and concentrated in vacuo. The crude oil was subjected to flash chromatography (eluent: ethyl acetate/hexanes) to yield 22%. ^{1}H NMR (400 MHz, $CDCl_3$): δ 6.90 (s, 2H, arom.), 5.14 (s, 1H, −OH), 4.98 (d, 1H, J = 8.0 Hz, 1H, −NH), 4.60−4.55 (m, 1H, −CH), 3.74 (s, 3H, $-OCH_3$), 3.03 (d, J = 5.6 Hz, 2H, CH_2), 1.44 (s, 27H, 3 × $-C(CH_3)_3$) ppm. ^{13}C NMR (100 MHz, $CDCl_3$): δ 172.54, 155.03, 152.82, 135.88, 126.32, 125.89, 79.74, 54.43, 52.15, 37.96, 34.25, 30.31, 28.36 ppm. HRMS (ES+) calculated (M) 408.2749, observed 408.2737.

Determination of pK_a's of the Tyrosine Analogues by UV Spectroscopy. A buffer solution of 10 mM potassium phosphate and 200 mM KCl was adjusted to the desired pH using 1 M KOH or 1 M HCl in the range of pH 2−14. The buffer solution (2 mL) was transferred to a cuvette, and a blank UV spectrum was recorded. To this solution was added the solution of amino acid in absolute ethanol (25 mM, 4 μL), and the UV spectrum was recorded and the pH remeasured. The absorption at the wavelength of maximum absorption for the aryloxide ion was used to determine the fraction of amino acid in its aryloxide ion form, $f_{aryloxide}$, using eq 1, where A is the absorbance at λ_{max}.

$$f_{aryloxide} = \frac{A(pH) - A(pH_{low})}{A(pH_{high}) - A(pH_{low})} \quad (1)$$

Plotting the values of $f_{aryloxide}$ as a function of pH resulted in the familiar titration curve, which was fit to eq 2 to obtain the pK_a.

$$f_{aryloxide} = \left(\frac{10^{(pH-pKa)}}{1 + 10^{(pH-pKa)}}\right) \quad (2)$$

Anodic Peak Potentials of Tyrosine and Its Analogues by Differential Pulse Voltammetry. Voltammagrams were obtained using an Electrochemical Analyzer from CH Instruments. The experiments were performed in a glass cell with three electrodes. The working electrode was glassy carbon and was polished using 0.05 μm alumina powder before each measurement. The reference electrode was an Ag/AgCl reference electrode, and the counter electrode was a platinum wire. The buffer solution, 10 mM potassium phosphate containing 3 M KCl as supporting electrolyte, was adjusted to the desired pH using 1 M KOH or 1 M HCl in the range of pH 6−8.5. To 2 mL of buffer solution was added the solution of amino acid in absolute ethanol (25 mM, 10 μL), and the pH was remeasured. The solutions were continuously sparged to remove oxygen. Under these conditions, in buffered solutions of pH 7.0 (25 mM NaH_2PO_4/Na_2HPO_4), the reversible $Fe(CN)_6^{3-/4-}$ couple was +203 mV versus the Ag/AgCl, which allows potentials to be calculated versus NHE[24] by adding 204 mV to the peak potentials in Figure 2. Voltammetry parameters: initial potential = 0 V, final potential = 1 V, pulse width = 0.05 s, pulse period = 0.2 s.

EPR Spectra of the Tyrosyl Radical and Its Analogues. Radicals were generated at 298 K by irradiation of the sample with a 500 W high-pressure Hg-lamp directly in the spectrometer cavity, equipped with a quartz Dewar, controlled by a Bruker B-VT100 variable temperature unit. The actual temperature inside the cavity was monitored before and after each experiment with a Delta OHM HD9218 type K thermocouple and was stable within ±0.1 °C. Samples, prepared in 4.0 mm i.d. suprasil quartz tubes and consisting of doxygenated benzene solutions of di-*tert*-butylperoxide (10% v/v M) containing the protected aminoacids **9**−**15** at various concentration, were photolyzed inside the cavity (vide infa), and spectra were collected. Digitized spectra were subjected to cepstral analysis and autocorrelation numerical approaches to obtain initial values of HSC, which were subsequently used in interactive fitting with computer simulated spectra, using Monte Carlo method. The software used both for numerical analysis and for simulation was SIMESR developed at the University of Bologna by Prof Marco Lucarini. HSC values were assigned by analogy with know phenoxyl,[15] pyridinoxyl,[11c] and pyrimidinoxyl[11c] radicals.

Determination of O−H BDEs of Tyrosine and Its Analogues. A deoxygenated benzene solution containing the compound under investigation (0.01−1 M), the appropriate reference phenol (0.01−0.2 M), and di-*tert*-butyl peroxide (0.1M) was sealed under nitrogen in a suprasil quartz EPR tube sitting inside the thermostatted cavity of an EPR spectrometer. Photolysis was carried out by focusing the unfiltered light from a 500 W high-pressure mercury

(24) O'Reilly, J. E. *Biochim. Biophys. Acta* **1973**, *292*, 509.

lamp on the EPR cavity. With compounds originating relatively persistent radical species (i.e., aryloxyl radicals showing no decay during an EPR fieldsweep), a short (1−5 s) UV pulse was used, while with the less persistent radicals continuous photolysis was necessary to establish "radical buffer"conditions.[15] The temperature was controlled with a standard variable temperature accessory and was monitored before and after each run. Relative radical concentrations were determined by comparison of the digitized experimental spectra with computer simulated ones. An iterative least-squares fitting procedure based on the systematic application of the Monte Carlo method was performed constraining the spectral parameters to a limited variation, while varying their relative intensities. At least three different initial concentration ratios of the two equilibrating species were investigated for each compound, and at least three determinations were obtained for each concentration. To ensure that equilibrium was established, different irradiation intensities were obtained by intercepting the UV-light with calibrated metal sectors.

Acknowledgment. We are grateful for the support of the Natural Sciences and Engineering Research Council of Canada, Ontario Ministry of Innovation and Queen's University. D.A.P. also acknowledges the support of the Canada Research Chairs program. L.V. and G.F.P. acknowledge financial support from MURST (Rome, Italy) and from the University of Bologna (Italy). We are grateful to Prof M. Lucarini (Bologna) for access to the EPR analysis/simulation software.

Supporting Information Available: Further synthetic details and associated characterization, ^{1}H and ^{13}C NMR spectra of key compounds, titration curve and pH-dependent potentials for **15**, sample EPR spectra, and associated simulations. This material is available free of charge via the Internet at http://pubs.acs.org.

JA907921W